Efficient On-Demand UAV Deployment and Configuration for Off-Shore Relay Communications

Sanghai Guan*, Jingjing Wang*, Chunxiao Jiang†, Xiangwang Hou*, Zhengru Fang*, and Yong Ren*‡
*Department of Electronic Engineering, Tsinghua University, Beijing, 100084, China
† Tsinghua Space Center, Tsinghua University, Beijing, 100084, China
‡ Peng Cheng Laboratory, Shenzhen, 518055, China

***Abstract*—At present, the development and exploration of the ocean are blossoming, but the maritime communication coverage still remains limited. By deploying unmanned aerial vehicle (UAV) mounted relay nodes between shore base stations and vessel users, the off-shore communication coverage and transmission efficiency can be substantially enhanced. Considering the specific transmission characteristics of air-sea and of air-shore channels and time-varying traffic of maritime information services, we formulate a minimum-maximization optimization problem of link capacity, where both the deployment of UAV-mounted relay node and the configuration of communication resources are optimized. To address this non-convex problem, we propose a particle swarm based algorithm, which is capable of three-dimensional position, antenna direction and time slot allocation scheme joint optimization. The simulation results demonstrate the high efficiency and reliability of our proposed algorithm in diverse off-shore relay scenarios with different coastal environments, vessel distributions and network traffic.**

***Index Terms*—UAV, off-shore relay communications, optimal deployment, resource configuration, particle swarm optimization.**

I. Introduction

In recent years, the development and exploration have attracted increasing attention from the world. A wide-area and high-rate maritime information coverage undoubtedly becomes a critical supporting condition for marine industries. According to statistics, most vessels sail within 50 kilometers from the coast. However, the terrestrial mobile communication base stations only cover a few kilometers, making most of the off-shore vessel users cannot access the terrestrial network directly [1]. At present, the airborne relay base stations represented by UAVs are widely applied for flexible deployment, low cost and wide coverage [2]. On the one hand, the UAVs can be freely deployed in three-dimensional (3D) space, which can adapt to the mobility of users and improve the flexibility of network configuration. On the other hand, the communication link from air to ground or sea surface is conducive to avoiding obstacles and establishing the line-of-sight (LoS) communication link, reducing the loss and achieving higher capacity and lower power consumption. Therefore, deploying the UAV relay node between the shore base station and vessel users and establishing an off-shore relay communication system becomes a feasible way to provide high-rate and low-cost information service for a majority of off-shore vessel users.

Nowadays, growing attention has been paid to the deployment and configuration problem of relay nodes. The main research fields include energy, reliability and delay aware dynamic resource allocation and optimization. Specifically, Fang *et al.* [3] investigated a multi-AUV assisted heterogeneous underwater information collection scheme for the optimization of age of information (AoI). Hou *et al.* [4] introduced both partial computation offloading and reliable task allocation with a reprocessing mechanism to Internet of Vehicles (IoV). Xue *et al.* [5] studied the joint 3D position and transmission power optimization problem to maximize the network capacity. Wang *et al.* [6] investigated the secure communication rate maximization problem under interference and eavesdropping. Moreover, a pair of joint trajectory planning and transmission power control methods are proposed by Zeng *et al.* [7] and Zhang *et al.* [8] to maximize the throughput and reliability of the relay system, respectively. In [9], Chen *et al.* investigated the optimal height of UAV relay nodes under different network reliability metrics.

However, these works are mainly focused on terrestrial relay systems, while the designing of off-shore relay system faces more challenges [10]. Firstly, due to the complicated off-shore environment, wireless communication is interfered by obstacles on the shore as well as the reflection of sea surface. Hence, we have to discuss and model the air-ground and air-surface links respectively and ensure the reliability of two links. In addition, the position of vessels always changes and their distributions are also diverse, so it is necessary to consider the efficiency of UAV deployment and the fairness of the users' quality of service (QoS). Finally, the uplink and downlink traffic of maritime communication is time-varying. For example, the multimedia service often needs a lot of communication resources allocated to the downlink, while the monitoring video needs many uplink communication resources. Hence, the channel resources need to be flexibly allocated on demand. Therefore, we aim to improve the transmission capacity based QoS of the relay system, by optimizing both the on-demand UAV relay node deployment and communication resource configuration [11]. The original contributions of this paper can be summarized as follows:

- An on-demand UAV deployment and configuration model is constituted for off-shore relay communications. Based on this model, we formulate a minimum-maximization optimization problem of link capacity to strike a balance between the transmission efficiency and service fairness.

- To solve the non-convex problem formulated, we conceive a particle swarm based algorithm for UAV 3D position, antenna direction and time slot allocation joint optimization for adapting the time-varying locations of vessels and the fluctuating network traffic.
- We evaluate our proposed algorithm in diverse off-shore relay scenarios associated with different coastal environments, vessel distributions and network traffic. Extensive simulation results verify its high efficiency and reliability.

The remaining content is arranged as follows. We introduce our off-shore relay system model and the problem formulation in Section II. Section III provides the heuristic joint optimization algorithm to realize efficient on-demand deployment and configuration of the UAV relay node. Simulation results based on different off-shore relay scenarios are shown in Section IV, followed by our conclusions in Section V.

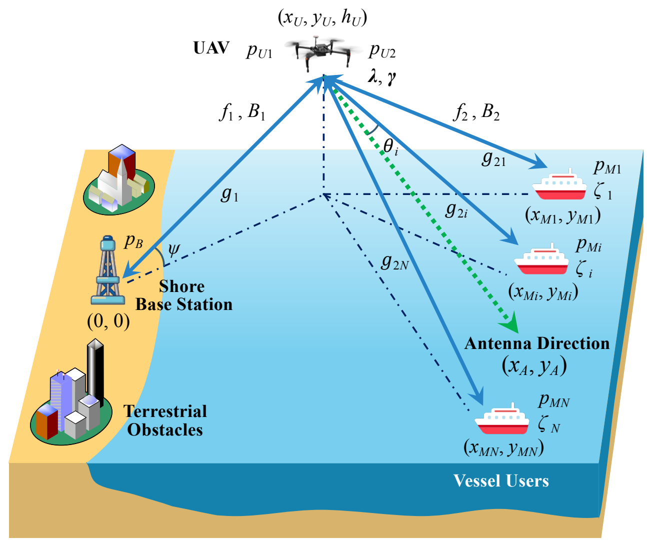

Fig. 1. UAV aided off-shore relay system.

II. System Model

A. Overview

As shown in Fig. 1, we consider an off-shore relay system associated with a shore base station (BS), a UAV relay node, and N vessels. The coordinate of the BS and N maritime vessel users are $(0,0),(x_{M1},y_{M1}),\ldots,(x_{MN},y_{MN})$, where we ignore the height of the base station and ship-borne antennas. While the 3D coordinate of the UAV is (x_U,y_U,h_U). The relay system operates in a time division duplex (TDD) forwarding mode. Concretely, it only supports one-way forwarding transmission for one single user at each time slot, and the uplink and downlink transmission of a link share the same frequency resource. The carrier frequency and bandwidth of the BS-UAV link and the UAV-vessel links are f_1, B_1 and f_2, B_2, respectively, where all the transmission between the UAV and N vessels also share the same frequency resource. Moreover, the UAV is equipped with two independent directional antennas for the communication with the BS and the vessels, respectively. For the UAV-vessel links, we use θ_i to represent the deflection angle between the UAV antenna direction and the ray from UAV to vessel i, while (x_A,y_A) is the intersection of UAV antenna direction and sea surface. The antenna transmitting power of BS, UAV to BS, UAV to vessels, and vessels are p_B, p_{U1}, p_{U2} and $p_{M1},\ldots,p_{MN}$, respectively. Besides, since the uplink and downlink traffic of vessel users are unbalanced, we use $\zeta_i \in [0,1]$ to denote the ratio between uplink traffic and all traffic of vessel user i, and let $\zeta=[\zeta_1,\ldots,\zeta_N]$. Similarly, $\lambda=[\lambda_1,\ldots,\lambda_N]$ and $\gamma=[\gamma_1,\ldots,\gamma_N]$ are used to represent the time slot allocation scheme in this TDD system. Specifically, λ_i represents the ratio between the time slots allocated to vessel i and all time slots, and $\sum_{i=1}^{N}\lambda_i=1$. While $\gamma_i \in [0,1]$ is the ratio between the uplink time slots and all time slots allocated to vessel i.

B. Channel Model

Let us continue by elaborating on the channel model from the perspectives of BS-UAV and UAV-vessel links respectively. Firstly, for the communication between the BS and the UAV, considering the terrestrial obstacles around the shore BS, we adopt a Bernoulli model [12] to describe the path loss. The probability of constructing a LoS link is:

$$\mathbf{P}_{\mathrm{LoS}}(\psi)=\frac{1}{1+a\exp\{-b(\psi-a)\}}, \tag{1}$$

where a and b are environment parameters. ψ (°) is the elevation angle between the link and ground surface, i.e.,

$$\psi=\arcsin(h_U/d_1). \tag{2}$$

where $d_1=\sqrt{x_U^2+y_U^2+h_U^2}$ is the Euclidean distance between the BS and the UAV, and the probability of non-line-of-sight (NLoS) link equals $\mathbf{P}_{\mathrm{NLoS}}(\psi)=1-\mathbf{P}_{\mathrm{LoS}}(\psi)$. The path loss of the LoS and NLoS links are expressed by:

$$\mathrm{PL}_{\mathrm{LoS}}(d_1,f_1)=\mathrm{FSPL}(d_1,f_1)+\eta_{\mathrm{LoS}}, \tag{3}$$

$$\mathrm{PL}_{\mathrm{NLoS}}(d_1,f_1)=\mathrm{FSPL}(d_1,f_1)+\eta_{\mathrm{NLoS}}, \tag{4}$$

respectively, where $\mathrm{FSPL}(d,f)$ is the free space path loss (dB) under distance d (km) and frequency f (MHz), i.e.,

$$\mathrm{FSPL}(d,f)=20\log_{10}d+20\log_{10}f+32.44, \tag{5}$$

while η_{LoS} and η_{NLoS} are the extra loss of LoS link and NLoS link respectively related to shore environments [13]. Hence the expected loss of the UAV-BS link is represented by:

$$\mathrm{PL}_1(d_1,f_1)=\mathrm{FSPL}(d_1,f_1)+\mathbf{P}_{\mathrm{LoS}}(\psi)\eta_{\mathrm{LoS}}+\mathbf{P}_{\mathrm{NLoS}}(\psi)\eta_{\mathrm{NLoS}}. \tag{6}$$

Therefore, the channel capacity (bits/s) of BS-to-UAV and UAV-to-BS links are:

$$C_{\mathrm{BU}}=B_1\log_2(1+g_1p_B/\sigma^2), \tag{7}$$

$$C_{\mathrm{UB}}=B_1\log_2(1+g_1p_{U1}/\sigma^2), \tag{8}$$

respectively, where the channel gain $g_1=10^{-\mathrm{PL}_1/10}$ and σ^2 is the variance of additive white Gaussian noise (AWGN).

Then, for the communication between the UAV and vessels, there are some empirical path loss models that can be adopted [14]. The path loss of the transmission between air and sea surface can be described by:

$$\mathrm{PL}_{2i} = 10n\log_{10}(d_{2i}) + \eta_M(f_2) + \eta_A(\theta_i). \tag{9}$$

Specifically, the first two items of (9) are the empirical air-sea path loss [15], which is usually close to free space path loss. n is the path loss factor which is usually in $[1,3]$, and η_M is the empirical extra loss corresponding to the carrier frequency. Then, the last item of (9) is the directivity loss caused by the antenna direction deflection [16] and equals:

$$\eta_A(\theta_i) = \min\left\{12\left(\theta_i/15^\circ\right)^2,\ 20\mathrm{dB}\right\}. \tag{10}$$

Hence, the channel capacity (bits/s) of UAV-to-vessel-i and vessel-i-to-UAV links are:

$$C_{\mathrm{UM}i} = B_2\log_2(1 + g_{2i}\,p_{U2}/\sigma^2), \tag{11}$$

$$C_{\mathrm{MU}i} = B_2\log_2(1 + g_{2i}\,p_{Mi}/\sigma^2), \tag{12}$$

respectively, where the channel gain $g_{2i} = 10^{-\mathrm{PL}_{2i}/10}$. Moreover, in this TDD system, the actual link capacity is scaled by the time slots allocated. For example, the actual capacity of the uplink transmission from vessel i to UAV is $\lambda_i\gamma_i C_{\mathrm{MU}i}$.

C. Problem Formulation

Based on the above discussions, we formulate the UAV deployment and configuration problem as follows:

$$\max_{(x_U,y_U,h_U),(x_A,y_A),\lambda,\gamma} \quad C, \tag{13a}$$

$$\text{s.t.}\quad C_i^{\mathrm{ul}} = \min\{C_{\mathrm{MU}i}, C_{\mathrm{UB}}\},\ \ \forall i\in\mathbb{I}, \tag{13b}$$

$$C_i^{\mathrm{dl}} = \min\{C_{\mathrm{BU}}, C_{\mathrm{UM}i}\},\ \ \forall i\in\mathbb{I}, \tag{13c}$$

$$C_i = \min\left\{\frac{\lambda_i\gamma_i C_i^{\mathrm{ul}}}{\zeta_i}, \frac{\lambda_i(1-\gamma_i)C_i^{\mathrm{dl}}}{1-\zeta_i}\right\}, \forall i\in\mathbb{I}, \tag{13d}$$

$$C = \min\{C_1,\ldots,C_N\}, \tag{13e}$$

$$[x_{\min}, y_{\min}, h_{\min}] \preceq [x_U, y_U, h_U] \preceq [x_{\max}, y_{\max}, h_{\max}], \tag{13f}$$

where $\mathbb{I} = \{1,\ldots,N\}$ is the index set of the vessels, and the constraints of this problem concern the following four aspects.

1) *Link Capacity Balance*: As shown in (13b) and (13c), the capacity of the entire BS-UAV-vessel link is determined by either the BS-UAV or the UAV-vessel link which is associated with a smaller capacity.
2) *Uplink-Downlink Traffic Balance*: In this TDD system, the actual reachable data rate of uplink and downlink for vessel i are $\lambda_i\gamma_i C_i^{\mathrm{ul}}$ and $\lambda_i(1-\gamma_i)C_i^{\mathrm{dl}}$, respectively. As a result, considering users' actual uplink traffic ratio ζ, we use (13d) to achieve the consistency between the uplink/downlink transmission capacity and the actual uplink/downlink traffic. Then we use the traffic-normalized total link capacity C_i to describe the actual maximum reachable data rate based QoS of vessel i.
3) *Multi-User Service Fairness*: Considering the QoS C_i of different vessel users is different, we take the vessels' minimum QoS C as the optimization object as (13e), and formulate a minimum-maximization problem to guarantee the service fairness for all vessel users.
4) *UAV Deployment Safety*: As shown in (13f), the deployable sea area and hovering altitude of the UAV are limited to a specific space to ensure flight safety.

III. Particle Swarm Optimization Based Solution

To tackle the non-convexity of this problem, we conceive a particle swarm optimization (PSO) based algorithm as summarized in Algorithm 1, where we generate several random variables called *particles* in the solution space and compose a *particle swarm* [17]. The particle swarm finds the optimal solution of the problem through swarm interaction and iterative search.

Algorithm 1: PSO Based Joint Solution Method

Input Particle swarm size S, number of iterations T, parameters of the system model and the algorithm;
Initialization Particle position $z_1,\ldots,z_S$, particle velocity $v_1,\ldots,v_S$, particle fitness value $q_1,\ldots,q_S$;
for $t = 1,\ldots,T$ **do**
  for $j = 1,\ldots,S$ **do**
    Update particle velocity $v_j \Leftarrow \omega_t v_j + s_1 r_1(z_j^\star - z_j) + s_2 r_2(z^\star - z_j)$;
    Update particle position $z_j \Leftarrow z_j + v_j$;
    Adjust z_j if it is out of the feasible region;
    Calculate particle fitness value q_j;
    Update history best position $z_j^\star$, history best fitness value $q_j^\star$;
  end
  Update global best position $z^\star$, global best fitness value $q^\star$;
end
Output Optimum solution $(x_U^\star, y_U^\star, h_U^\star)$, $(x_A^\star, y_A^\star)$, $\lambda^\star$, $\gamma^\star$, optimum system QoS $C^\star$.

Firstly, after setting the number iteration T and the size of particle swarm S. We randomly generate S particles in the feasible region of this problem. The particle has two attributes, i.e., *particle position* and *particle velocity*. The position of particle j is represented as:

$$z_j = [x'_{Uj}, y'_{Uj}, h'_{Uj}, x'_{Aj}, y'_{Aj}, \lambda_j, \gamma_j], \tag{14}$$

where $\lambda_j = [\lambda_{1j},\ldots,\lambda_{Nj}]$ and $\gamma_j = [\gamma_{1j},\ldots,\gamma_{Nj}]$. Here we adopt a normalized coordinate as:

$$x'_{Uj} = (x_{Uj} - x_{\min})/(x_{\max} - x_{\min}), \tag{15}$$

to represent the relationship between the particle position and the UAV deployment coordinate for the convenience of deduction, which is similar to y'_{Uj}, h'_{Uj}, x'_{Aj}, and y'_{Aj}. Here we also limit the range for antenna direction $x_{Aj} \in [x_{A\min}, x_{A\max}]$ and $y_{Aj} \in [x_{A\min}, x_{A\max}]$ without loss of generality. In the initialization step, we generate random values in $[0,1]$ for normalize deployment coordinate $x'_{Uj}, y'_{Uj}, h'_{Uj}$, antenna direction x'_{Aj}, y'_{Aj}, and users' uplink time slot ratio γ_j, for $j = 1,\ldots,S$.

Then we randomly generate time slot allocation ratio λ_j for $j = 1, \ldots, S$ under the constraint of:

$$\{\lambda_j \,|\, \sum_{i=1}^{N} \lambda_{ij} = 1, 0 \preceq \lambda_j \preceq 1\}, \tag{16}$$

which is a convex region on a hyper plane. Moreover, the velocity of particle j is represented as v_j with the same size of z_j. Similarly, we can generate random value in $[-0.2, 0.2]$ for all dimensions except λ_j in the initialization. Specially, for the dimensions of time slot allocation ratio λ_j, we also have to ensure the velocity in these dimensions parallel to the plane described in (16), which can be obtained by subtract two points on it. Moreover, the system QoS C in our model corresponding to the particle position $z_1, \ldots, z_S$ is called *particle fitness value* in PSO algorithm, represented by $q_1, \ldots, q_S$. Because a particle's position changes in each iteration step, the position on its trace with the highest fitness value is called its *history best position*. The history best position and corresponding *history best fitness value* of particle j are represented by $z_i^\star$ and $q_j^\star$, respectively. The history best fitness value of the whole particle swarm is called the *global best fitness value* $q^\star = \max\{q_1^\star, \ldots q_S^\star\}$, whose corresponding *global best position* is represented by $z^\star$.

Then, in each iteration step t, the position and velocity of the particle swarm are updated. The update strategy of particle velocity is expressed as:

$$v_j = \omega_t v_j + r_1 s_1 (z_j^\star - z_j) + r_2 s_2 (z^\star - z_j), \tag{17}$$

where r_1 and r_2 are random values in $[0, 1]$, while s_1 and s_2 are history and global learning factors in $[0, 4]$. ω_t is the inertial factor changing with iteration step t as:

$$w_t = (w_1 - w_T)(T - t)/t + w_T, \tag{18}$$

where w_1 and w_T in $[0, 1]$ are specified inertial factor for the first and last iteration step. It is usually set $w_1 > w_T$ to realize the balance of exploration and convergence performance. Then the particle position z_j is updated as:

$$z_j = z_j + v_j. \tag{19}$$

For the particle moving out of the feasible region, we adjust it to the intersection of its trace and the border of feasible region. Base on the fitness value q_j of z_j, the history best position $z_j^\star$ and history best fitness value $q_j^\star$ are also updated. At the last of each iteration, we update global best position $z^\star$ and global best fitness value $q^\star$. Lastly, based on global best position $z^\star$, we can obtain the optimum solution including optimum deployment coordinate $(x_U^\star, y_U^\star, h_U^\star)$, optimum antenna direction $(x_A^\star, y_A^\star)$ and optimum time slot allocation scheme $\lambda^\star$, $\gamma^\star$, as well as the optimum system QoS $C^\star = q^\star$.

IV. Simulation Results

In simulations, we consider an off-shore relay system with five vessels with the distribution as shown in Fig. 2, where the coordinates of vessel 3 in the center and the other vessels around it are $(l_1, 0)$ and $(l_1 \pm l_2/\sqrt{2}, \pm l_2/\sqrt{2})$, respectively. Other default simulation parameters of the relay system model and the algorithm are summarized in Table I. Moreover, we consider two kinds of shore environment, i.e., suburban and urban from the ITU standardized model, with different LoS probability factors and extra loss of the BS-UAV link.

TABLE I
Default Simulation Parameters

Symbol	Description	Value
N	Number of vessels	5
f_1, f_2	Carrier frequency	2GHz, 5.8GHz
B_1, B_2	Bandwidth	250kHz, 250kHz
p_B, p_{U1}, p_{U2} $p_{M1}, \ldots, p_{MN}$	Transmitting power	10W, 5W, 5W 2W
σ^2	AWGN power density	–174dB/Hz
$\zeta_1, \ldots, \zeta_N$	Uplink traffic ratio	0.1, 0.3, 0.5, 0.7, 0.9
a, b	BS-UAV LoS probability factor	4.88, 0.429 (Suburban) 9.61, 0.158 (Urban)
$\eta_{\rm LoS}$, $\eta_{\rm NLoS}$	BS-UAV extra loss	0.1dB, 21dB (Suburban) 1dB, 20dB (Urban)
n	UAV-vessel loss factor	1.6
η_M	UAV-vessel extra loss	109.8dB
$x_{\min}, x_{\max}$ $y_{\min}, y_{\max}$ $h_{\min}, h_{\max}$	UAV safety deployment range	0km, 30km -10km, 10km 1km, 10km
$x_{A\min}, x_{A\max}$ $y_{A\min}, y_{A\max}$	UAV antenna direction range	0km, 30km -10km, 10km
l_1, l_2	Vessel distance	20km, 1km
S	Particle swarm size	500000
T	Number of iterations	100
s_1, s_2	Learning factor	2, 2
w_1, w_T	Inertial factor	0.7, 0.4

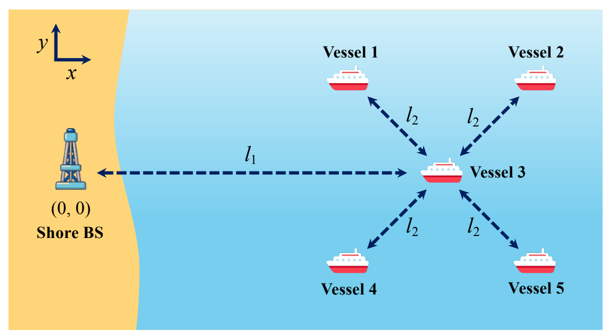

Fig. 2. Distribution of vessels in simulation.

Firstly, we verify the convergence of our proposed algorithm. Fig. 3 shows the position of the particle swarm when iteration step $t = 50$ and $t = 100$ under the assumption of urban shore environment. It can be found that the deployment coordinate shown in Fig. 3(a) and Fig. 3(b), the antenna direction coordinate shown in Fig. 3(c) and Fig. 3(d), as well as the mean value and standard deviation of time slot allocation scheme shown in Fig. 3(e) to Fig. 3(h) all converge to the optimal solution. As to the optimal deployment, $(x_U^\star, y_U^\star, h_U^\star)$ is about $(11.0, 0, 4.9)$ km and $(x_A^\star, y_A^\star)$ equals to $(19.9, 0)$ km near the center of vessels. The optimal time slot allocation scheme is about $\lambda^\star = [0.193, 0.198, 0.199, 0.202, 0.208]$ and $\gamma^\star = [0.107, 0.317, 0.520, 0.715, 0.907]$. This is because the

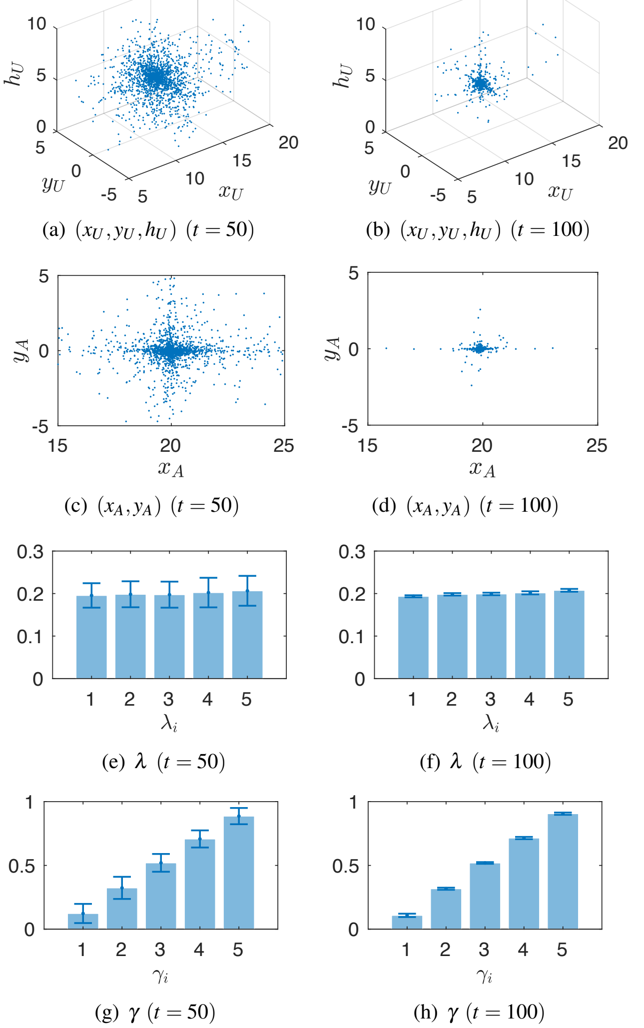

(a) (x_U, y_U, h_U) $(t=50)$ (b) (x_U, y_U, h_U) $(t=100)$

(c) (x_A, y_A) $(t=50)$ (d) (x_A, y_A) $(t=100)$

(e) λ $(t=50)$ (f) λ $(t=100)$

(g) γ $(t=50)$ (h) γ $(t=100)$

Fig. 3. Convergence performance of the joint optimization algorithm.

uplink transmission power p_{Mi} and p_{U1} are both lower than downlink transmission power p_{U2} and p_B in simulation, a few more time slots $\lambda_i^\star$ are allocated to vessels with higher uplink traffic ratio ζ_i, and $\gamma^\star$ are a little higher than ζ to strike a balance between uplink and downlink capacity.

Then, in order to evaluate the effectiveness of our model, we compared the performance of our joint optimization method and another reliability oriented partial optimization method under different vessel distribution parameters l_1 and l_2. In this partial optimization method, we fix UAV's plane position at the center of vessels $(x_U, y_U) = (l_1, 0)$, and fix the antenna direction vertical downward as $(x_A, y_A) = (l_1, 0)$. In order to realize a high LoS communication probability with the BS and a low antenna deflection with the vessels to construct high reliability links, the UAV is deployed at the altitude of:

$$h_U = \max\left\{l_1 \tan(20^\circ), l_2/\tan(15^\circ)\right\}. \tag{20}$$

Based on the settings above, we partially optimize UAV's time slot allocation ratio λ and uplink time slot allocation

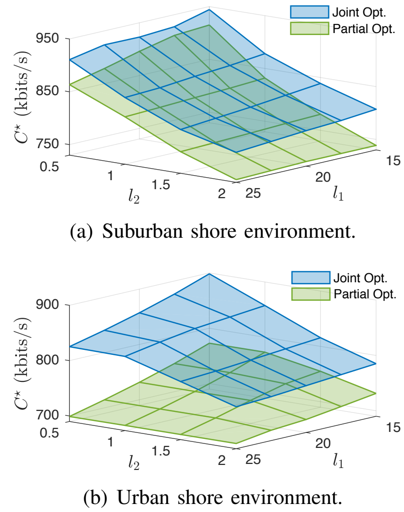

(a) Suburban shore environment.

(b) Urban shore environment.

Fig. 4. Performance of our proposed joint optimization method and the reliability oriented partial optimization method.

ratio γ by PSO algorithm for comparison. As the simulation results based on suburban and urban shore environments shown in Fig. 4, our joint optimization method overwhelms the partial optimization method, and improves the service capacity based system QoS by 7% and 12% in average, respectively. Moreover, we can find that the system QoS $C^\star$ decreases with the increasing of l_1 and l_2, and the system QoS $C^\star$ under urban shore environment is lower than that of suburban shore environment. Hence, we can conclude that long relay distance, sparse vessel distribution and dense shore obstacles are adverse to off-shore UAV relay communications.

Lastly, we further investigate the relationship between the optimum UAV deployment scheme and simulation scenarios. Fig. 5(a) reveals the relationship between the optimal horizontal coordinate $x_U^\star$ and l_1, l_2. It can be found that when the distance between vessels l_2 is fixed, $x_U^\star$ increases uniformly with relay distance l_1. When the vessels' distance l_2 increases, the optimum deployment scheme tends to shorten $x_U^\star$ and extend the distance to vessels, which is conductive to narrow the antenna deflection angle θ_i between vessels and reduce loss $\eta_A(\theta_i)$. In addition, compared to the suburban shore environment, the distance between the UAV and BS under the urban shore environment is closer, for decreasing the path loss PL_1 as well as increase the elevation angle ψ and the LoS transmission probability $\mathbf{P}_{\text{LoS}}$ at the same time. In addition, Fig. 5(b) reflects the variation of optimum deployment height $h_U^\star$. It is obvious that $h_U^\star$ increases with the increasing of l_1 and the decreasing of l_2, and the reason is similar to aforementioned $x_U^\star$. Meanwhile, $h_U^\star$ of the urban shore environment is significantly higher than that of suburban shore environment to achieve stable LoS communication with the BS, but it increases the loss of two links and results in the degradation of system QoS $C^\star$. To elaborate a little further, Fig. 5(c) shows the BS-UAV transmission elevation angle ψ under the optimal solution. It can be found that ψ increases slightly with the increase of l_1 and the decrease of

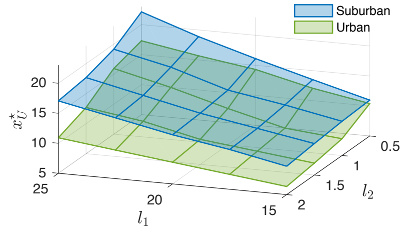

(a) Optimum horizontal position $x_U^\star$.

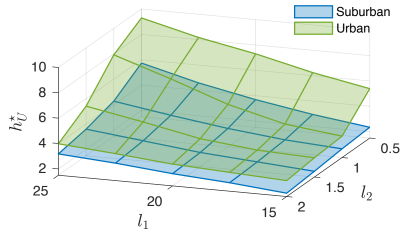

(b) Optimum height $h_U^\star$.

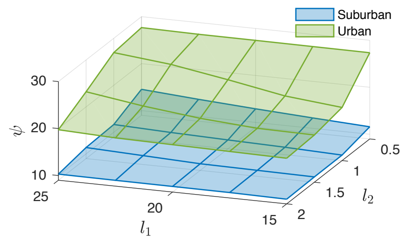

(c) BS-UAV elevation angle ψ under $(x_U^\star, y_U^\star, h_U^\star)$.

Fig. 5. The optimum deployment position versus l_1 and l_2.

l_2, which equals about 10° to 15° and 20° to 30° for suburban and urban shore environments, respectively. Because longer vessels' distance l_2 leading to a larger antenna deflection angle θ_i, the optimum solution tends to reduce ψ and h_U to alleviate it, at the cost of lower LoS transmission possibility $\mathbf{P}_{\mathrm{LoS}}$, which reflects the balance between two links in our model. These conclusions are conductive to the design and optimization of off-shore relay communication systems.

V. Conclusions

In this paper, we proposed a UAV aided off-shore TDD relay system model and analyzed the air-shore and air-sea transmission characteristics. Moreover, we took link capacity balance, uplink-downlink traffic balance, UAV deployment safety as well as the service fairness for all vessel users into consideration, and formulated it into a minimum-maximization optimization problem to adapt with the features of off-shore communication. Furthermore, the particle swarm based algorithm for deployment coordinate, antenna direction, and time slot allocation joint optimization improved the solving efficiency of UAV deployment and configuration scheme. Sufficient simulations based on several off-shore scenarios with different shore environments, relay distance, vessel distributions, and uplink-downlink traffic proved the effectiveness of our model and the joint optimization method.

VI. Acknowledgement

This work of Dr. Wang was partly supported by National Natural Science Foundation of China (Grant No. 62071268), and partly supported by China Postdoctoral Science Foundation (Grant No. 2020T130357). Moreover, this work is also supported in part by the Project 'The Verification Platform of Multi-Tier Coverage Communication Network for Oceans (LZC0020)' of Peng Cheng Laboratory.

References

[1] W. Chen, J. Yang, J. Ma, and S. Li, "New developments in maritime communications: A comprehensive survey," *China Commun.*, vol. 9, no. 2, pp. 31–42, 2012.

[2] J. Wang, C. Jiang, H. Zhu, R. Yong, R. G. Maunder, and L. Hanzo, "Taking drones to the next level: Cooperative distributed unmanned-aerial-vehicular networks for small and mini drones," *IEEE Veh. Technol. Mag.*, vol. 12, no. 3, pp. 73–82, 2017.

[3] Z. Fang, J. Wang, C. Jiang, Q. Zhang, and Y. Ren, "AoI inspired collaborative information collection for AUV assisted internet of underwater things," *IEEE Internet of Things Journal, (DOI: 10.1109/JIOT.2021.3049239)*, Jan. 2021.

[4] X. Hou, Z. Ren, J. Wang, W. Cheng, Y. Ren, K. C. Chen, and H. Zhang, "Reliable computation offloading for edge-computing-enabled software-defined IoV," *IEEE Internet of Things Journal*, vol. 7, no. 8, pp. 7097–7111, 2020.

[5] Z. Xue, J. Wang, G. Ding, and Q. Wu, "Joint 3D location and power optimization for UAV-enabled relaying systems," *IEEE Access*, vol. 6, pp. 43 113–43 124, 2018.

[6] Q. Wang, Z. Chen, W. Mei, and J. Fang, "Improving physical layer security using UAV-enabled mobile relaying," *IEEE Wireless Commun. Lett.*, vol. 6, no. 3, pp. 310–313, 2017.

[7] Y. Zeng, R. Zhang, and T. J. Lim, "Throughput maximization for UAV-enabled mobile relaying systems," *IEEE Trans. Commun.*, vol. 64, no. 12, pp. 4983–4996, 2016.

[8] S. Zhang, H. Zhang, Q. He, K. Bian, and L. Song, "Joint trajectory and power optimization for UAV relay networks," *IEEE Commun. Lett.*, vol. 22, no. 1, pp. 161–164, 2018.

[9] Y. Chen, W. Feng, and G. Zheng, "Optimum placement of UAV as relays," *IEEE Commun. Lett.*, vol. 22, no. 2, pp. 248–251, 2018.

[10] D. Kidston and T. Kunz, "Challenges and opportunities in managing maritime networks," *IEEE Commun. Mag.*, vol. 46, no. 10, pp. 162–168, 2008.

[11] J. Wang, C. Jiang, H. Zhang, Y. Ren, K.-C. Chen, and L. Hanzo, "Thirty years of machine learning: The road to Pareto-optimal wireless networks," *IEEE Commun. Surveys Tut.*, vol. 22, no. 3, pp. 1472–1514, 2020.

[12] A. Al-Hourani, S. Kandeepan, and S. Lardner, "Optimal LAP altitude for maximum coverage," *IEEE Wireless Commun. Lett.*, vol. 3, no. 6, pp. 569–572, 2014.

[13] A. Al-Hourani and K. Gomez, "Modeling cellular-to-UAV path-loss for suburban environments," *IEEE Wireless Commun. Lett.*, vol. 7, no. 1, pp. 82–85, 2017.

[14] J. Wang, H. Zhou, Y. Li, Q. Sun, Y. Wu, S. Jin, T. Q. Quek, and C. Xu, "Wireless channel models for maritime communications," *IEEE Access*, vol. 6, pp. 68 070–68 088, 2018.

[15] D. W. Matolak and R. Sun, "Air–ground channel characterization for unmanned aircraft systems–Part I: Methods, measurements, and models for over-water settings," *IEEE Trans. Veh. Technol.*, vol. 66, no. 1, pp. 26–44, 2016.

[16] *Guidelines for evaluation of radio interface technologies for IMT–advanced*, International Telecommunication Union (ITU) Recommendation for Mobile, Radiodetermination, Amateur and Related Satellite Services, ITU-R M.2135-1, 2009.

[17] R. Poli, J. Kennedy, and T. Blackwell, "Particle swarm optimization: An overview," *Swarm Intell.*, vol. 1, no. 1, pp. 33–57, 2007.